Asian Journal of Control, Vol. 19, No. 3, pp. 1–13, May 2017
Published online in Wiley Online Library (wileyonlinelibrary.com) DOI: 10.1002/asjc.1461

STABLE DELAYED BILATERAL TELEOPERATION OF MOBILE MANIPULATORS

Diego D. Santiago, Emanuel Slawiñski, and Vicente A. Mut

ABSTRACT

This paper proposes a control scheme for a stable teleoperation of non-holonomic mobile manipulator robots. This configuration presents high-coupled dynamics and motion redundancy. The problem approached in this work is the teleoperation of the end effector velocity of the Mobile Manipulator, while system redundancy is used to achieve secondary control objectives. We considered variable asymmetric time delays as well as non-passive models of operator and environment. From this study, it is possible to infer the control parameters, depending on the time delay, in order to assure stability. Finally, the performance of the delayed teleoperation system is evaluated through simulations of human-in-the-loop internet teleoperation.

Key Words: Nonlinear control, bilateral teleoperation, delayed system, operational space control, null space control, mobile manipulator.

I. INTRODUCTION

Teleoperation allows the human operator to perform physical work remotely. These systems separate the user from the workspace, which can be hostile, dirty or even inaccessible [1]. Teleoperation of mobile robots and manipulators individually can achieve higher security and better performance of the task by using the intellectual and decision making capacity of the human operator [2]. Additionally the use of the Internet as a communication channel increases the applications of the teleoperation systems. However, the presence of time-delays can produce instability or low performance in a delayed teleoperation system [1,3,4] as well as poor transparency [5].

There are many control schemes for standard teleoperation between two manipulators including time delay [3,5,6]. The concept commonly used inside the design of control schemes for these systems is the injection of damping to dissipate kinetic energy in order to assure stability. Firstly, strategies like [7–9] add so-called apparent damping. Then, simple PD-like schemes plus injection of damping are used, achieving a stable operation, including position coordination [10–12] The literature involving teleoperation of mobile robots is less extensive but includes also a high diversity of strategies such as passivity-based controllers, impedence-based schemes, PD-like controllers and schemes based on wave variables [13]. One of the main reasons for an increased difficulty in applying existing proposals for mobile robot teleoperation is the mismatch between the models of the master and slave, for example if the master does not move, the mobile robot generally goes at a constant speed.

On the other hand, mobile manipulator teleoperation extends the capabilities of mobile robot and manipulators teleoperation allowing interaction with complex, unstructured environments and extending the workspace area. This is a relatively young research area. In these systems, motion redundancy complicates the controller design, especially when the master robot (usually 3DOF Joystick with force feedback) has less DOF than the mobile manipulator; therefore many research efforts are oriented to the human machine interface and redundancy resolution. In [14–16] switching control teleoperation is proposed, where the human operator decides to control mobile base speed or final effector position. In [17] a switching control teleoperation is developed, where the velocity of the end effector is controlled instead of the mobile base velocity. Although these works address the problem of bilateral teleoperation, the communication delays are considered negligible, therefore, the closed loop stability of the whole system, including the human operator is not analyzed.

In [18] and [19] a teleoperation approach using virtual spring and operational space formulation is proposed. Motion redundancy is used to reach secondary control objectives, and force feedback is also considered. In addition a stability proof is provided for small constant delays and assuming a passive behavior of the human operator. The strategies proposed for bilateral teleoperation of mobile manipulators, including time-varying delays and

Manuscript received October 29, 2015; revised August 9, 2016; accepted October 28, 2016.

The authors are with Instituto de Automática (INAUT), Universidad Nacional de San Juan. Av. Libertador San Martín 1109 (Oeste), J5400ARL San Juan, Argentina

D. Santiago is the corresponding author (e-mail: dsantiago@inaut.unsj.edu.ar).

stability analysis, are currently much less formalized than the pioneering areas mentioned and, therefore, the main motivation of this work is to apply the sophisticated background available in the state-of-the-art studies of bilateral teleoperation of robots (mobile and manipulator robots) to these systems in order to increase further the use of teleoperation systems in practice.

In contrast with most schemes available in the literature on mobile manipulator teleoperation, this paper proposes a control scheme that ensures the stability of the entire teleoperation loop, including a non-passive model of the human operator and the environment as well as non-negligible variables and asymmetric time delays. For this analysis no linearization techniques are used, instead delayed nonlinear systems analysis techniques are employed. Furthermore, an adjustment procedure for controller parameters is provided through which the designer can ensure the system stability and achieve a proper system performance.

The end effector velocity control is made with a PD-like plus damping scheme in task space, while the dynamics control and secondary control actions are achieved using the operation space formulation [20]. Furthermore, the scheme is evaluated with human-in-the-loop simulations and experimental teleoperations using the internet between Universidad Nacional de San Juan (UNSJ) San Juan Argentina and Universidade Federal do Espírito Santo (UFES) Victoria Brazil. These human-in-the-loop experiences are made in order to verify the theoretical analysis.

The paper is organized as follows: Section II presents some preliminary aspects such as the employed kinematic and dynamic models. In Section III a control scheme applied to bilateral teleoperation of no holonomic redundant mobile manipulator robots is proposed. In Section IV, the system stability is analyzed through a Lyapunov-Krasovskii functional (LKF). A method for adjusting system parameters is proposed in Section V. Section VI shows human-in-the-loop simulation and international teleoperation experimental results, where a user drives a robot simulator via the internet between two countries (Brazil–Argentina). Finally, in Section VII, the conclusions of this work are given.

II. SYSTEM MODELING

Notation. We use standard notations throughout the paper. If x is a scalar, $\mathbf{x}$ is a vector and is a matrix, then $|x|$ is the absolute value of, $\mathbf{x}^{\mathbf{T}}$ is the transpose of vector, $\mathbf{Z}^{\mathbf{T}}$ is the transpose of the matrix, $|\mathbf{y}|$ is the Euclidean norm of $\mathbf{y}$, $|\mathbf{Z}|$ is the induced norm of $\mathbf{Z}$, $\mathbf{Z} > 0 (\mathbf{Z} < 0)$ means that $\mathbf{Z}$ is positive definite (negative definite), and $\lambda_{\min}(\mathbf{Z})$,$\lambda_{\max}(\mathbf{Z})$ represent the minimum and maximum eigenvalue of matrix $\mathbf{Z}$. In addition, $||\mathbf{y}||_1$,$||\mathbf{y}||_2$ and $||\mathbf{y}||_\infty$ represent the L1-norm, L2-norm and L infinite-norm of respectively $\mathbf{y}$.

The dynamic model of the master device can be expressed in its traditional form:

$$\mathbf{M_m}(\mathbf{x_m})\ddot{\mathbf{x}}_\mathbf{m} + \mathbf{C_m}(\mathbf{x_m},\dot{\mathbf{x}}_\mathbf{m})\dot{\mathbf{x}}_\mathbf{m} + \mathbf{g_m}(\mathbf{x_m}) = \mathbf{f_m} + \mathbf{f_h} \quad (1)$$

where $\mathbf{x_m}, \dot{\mathbf{x}}_\mathbf{m}\ddot{\mathbf{x}}_\mathbf{m} \in \mathbb{R}^l$ are the position, velocity and acceleration of the master end effector in Cartesian space respectively; $\mathbf{M_m}(\mathbf{x_m}) \in \mathbb{R}^{l \times l}$ is the inertia matrix; $\mathbf{C_m}(\mathbf{x_m},\dot{\mathbf{x}}_\mathbf{m})$ is the matrix representing centripetal and Coriolis forces; $\mathbf{g_m}(\mathbf{x_m})$ is the gravitational force; $\mathbf{f_h}$ is the force and torques exerted by the human operator and $\mathbf{f_m}$ is the control force applied to the master in operational space.

For the Slave device, let us consider $\mathbf{q}(t) = [x \;\; y \;\; \phi \;\; \theta_1 \;\; \ldots \;\; \theta_k]^T \in \mathbb{R}^i$ the general coordinate system vector of the mobile manipulator formed by position and orientation of mobile platform $[x \quad y \quad \phi]^T$ and joint position of the k-DOF manipulator $[\theta_1 \quad \ldots \quad \theta_k]$.

Vectors $\mathbf{x_s}, \dot{\mathbf{x}}_\mathbf{s}\ddot{\mathbf{x}}_\mathbf{s} \in \mathbb{R}^n$ are the position, velocity and acceleration of the slave end effector in task space respectively. Vector $\mathbf{x_s}$ may be composed of position and orientation of the slave manipulator end-effector in terms of global frame.

The relation between $\dot{\mathbf{x}}_\mathbf{s}$and $\dot{\mathbf{q}}$is given by task Jacobian $\mathbf{J_q}(\mathbf{q}) \in \mathbb{R}^{n \times i}$.

$$\dot{\mathbf{x}}_\mathbf{s} = \mathbf{J_q}(\mathbf{q})\dot{\mathbf{q}} \quad (2)$$

Let us assume a non-holonomic velocity constraint of the mobile platform defined by,

$$\dot{x}\sin(\phi) - \dot{y}\cos(\phi) - a\dot{\phi} = 0 \quad (3)$$

where $\dot{x},\dot{y},\dot{\phi}$ are the velocity components of the mobile platform and a the distance between the mass and rotation center. This constrain can be written as

$$\mathbf{A}(\mathbf{q})\dot{\mathbf{q}} = 0 \quad (4)$$

where, $\mathbf{A}(\mathbf{q}) = [\, \sin(\phi) \quad -\cos(\phi) \quad -a \quad \mathbf{0_{1\times k}} \,]$.

We define $\mathbf{S}(\mathbf{q})$ as a matrix composed of a base vector of the null space of $\mathbf{A}(\mathbf{q})$, so equation (4) and (2) can be written as follows:

$$\dot{\mathbf{q}} = \mathbf{S}(\mathbf{q})\boldsymbol{\nu} \quad (5)$$

$$\dot{\mathbf{x}}_\mathbf{s} = \mathbf{J_q}\mathbf{S}\boldsymbol{\nu} \quad (6)$$

where $\boldsymbol{\nu} \in \mathbb{R}^m$with $m < i$ may be composed of angular and linear velocity of the mobile platform or its joint velocities, in conjunction with the joint velocities of the manipulator robot. From (6), the redefined system Jacobian is.

$$\mathbf{J} = \mathbf{J_q}\mathbf{S} \in \mathbb{R}^{n \times m} \quad (7)$$

In the following, we will use the expression of the end effector acceleration, which is obtained deriving (6)

$$\ddot{\mathbf{x}}_\mathbf{s} = \mathbf{J}\dot{\boldsymbol{\nu}} + \dot{\mathbf{J}}\boldsymbol{\nu} \quad (8)$$

The dynamic model of the mobile manipulator can be obtained from Lagrange's dynamic equation [(21)].

For n-DOF redundant manipulator mounted on a non-holonomic mobile platform, the dynamics consists of the coupled dynamics of the mobile platform and the manipulator [22,23]:

$$\mathbf{M_s(q)}\ddot{\mathbf{q}}+\mathbf{C_s}(\mathbf{q},\dot{\mathbf{q}})\dot{\mathbf{q}}+\mathbf{g_s(q)}=\mathbf{B(q)}\boldsymbol{\tau}_\mathbf{s}+\boldsymbol{\tau}_\mathbf{e}-\mathbf{A(q)}^\mathbf{T}\boldsymbol{\lambda} \tag{9}$$

$\mathbf{M_s(q)}\in\mathbb{R}^{i\times i}$is a symmetrical positive defined matrix that represents system inertia, $\mathbf{C_s}(\mathbf{q},\dot{\mathbf{q}})\dot{\mathbf{q}}\in\mathbb{R}^i$represents the components of centripetal and Coriolis forces.

Vector $\mathbf{g_s(q)}\in\mathbb{R}^{\ i}$represents the gravitational torques, $\mathbf{B(q)}$ is the transformation matrix of control actions, $\tau_\mathbf{s}$ is the torque input vector, $\tau_\mathbf{e}$ are the torques in the joint space caused by the environment interaction forces and $\mathbf{A(q)}^\mathbf{T}\lambda$ denotes a vector of non-holonomic constrain toques.

The unconstrained model of the mobile manipulator can be computed using equations (9) and (5).

$$\overline{\mathbf{M}}_\mathbf{s}(\mathbf{q})\dot{\nu}+\overline{\mathbf{C}}_\mathbf{s}(\mathbf{q},\dot{\mathbf{q}})\mathbf{v}+\overline{\mathbf{g}}_\mathbf{s}(\mathbf{q})=\boldsymbol{\tau}_\mathbf{c}+\boldsymbol{\tau}_\mathbf{ve} \tag{10}$$

where

$$\overline{\mathbf{M}}_\mathbf{s}(\mathbf{q})=\mathbf{S}^\mathbf{T}\mathbf{M}_\mathbf{s}(\mathbf{q})\mathbf{S}$$
$$\overline{\mathbf{C}}_\mathbf{s}(\mathbf{q},\dot{\mathbf{q}})=\mathbf{S}^\mathbf{T}\left[\mathbf{M}_\mathbf{s}(\mathbf{q})\dot{\mathbf{S}}+\mathbf{C}_\mathbf{s}(\mathbf{q},\dot{\mathbf{q}})\mathbf{S}\right]$$
$$\overline{\mathbf{g}}_\mathbf{s}(\mathbf{q})=\mathbf{S}^\mathbf{T}\mathbf{g}_\mathbf{s}(\mathbf{q})$$
$$\boldsymbol{\tau}_\mathbf{c}=\mathbf{S}^\mathbf{T}\mathbf{B}(\mathbf{q})\boldsymbol{\tau}_\mathbf{s}$$
$$\boldsymbol{\tau}_{ve}=\mathbf{S}^\mathbf{T}(\mathbf{q})\boldsymbol{\tau}_\mathbf{e}$$

The dynamically consistent generalized inverse $\mathbf{J}^+\in\mathbb{R}^{m\times n}$ was presented in [24], and corresponds to the solution that minimizes the manipulator instantaneous kinetic energy.

$$\mathbf{J}^+=\overline{\mathbf{M}}_\mathbf{s}^{\ -1}\mathbf{J}^\mathbf{T}\mathbf{M}_\mathbf{x} \tag{11}$$

Here $\mathbf{M_x(x_s)}$ is the inertia matrix of the model expressed in Cartesian coordinates, which for a redundant robot, under the assumption that $\mathbf{J}$ is full rank (that is, out of kinetics and representation singularities), can be written as follows

$$\mathbf{M}_\mathbf{x}=\left(\mathbf{J}\overline{\mathbf{M}}_\mathbf{s}^{\ -1}\mathbf{J}^\mathbf{T}\right)^{-1} \tag{12}$$

Note that as $m\geq n$, $\mathbf{J}^+$ is right inverse of $\mathbf{J}$, so the following identities hold

$$\mathbf{J}\mathbf{J}^+=\mathbf{J}^{+\mathbf{T}}\mathbf{J}^\mathbf{T}=\mathbf{I} \tag{13}$$

The relationship of torques in joint space $\boldsymbol{\tau}$ and forces in operational space $\mathbf{f}$ is given by:

$$\mathbf{f}=\mathbf{J}^{+\mathbf{T}}\boldsymbol{\tau} \tag{14}$$

Because $\mathbf{J}^{+\mathbf{T}}$ is redundant, the inverse operation is not unique. A general solution is

$$\boldsymbol{\tau}=\mathbf{J}^\mathbf{T}\mathbf{f}+\mathbf{N}^\mathbf{T}\boldsymbol{\tau}_0 \tag{15}$$

where $\boldsymbol{\tau}_0$ is an arbitrary vector and $\mathbf{N}^\mathbf{T}$ is the dynamically consistent null space of $\mathbf{J}^{+\mathbf{T}}$, which can be represented by

$$\mathbf{N}^\mathbf{T}=\mathbf{I}-\mathbf{J}^\mathbf{T}\mathbf{J}^{+\mathbf{T}} \tag{16}$$

In this article the following properties of dynamic models of master and slave devices are used [21]:

Property 1. The inertia matrices $\mathbf{M_m(x_m)}, \mathbf{M_s(q)}$ are symmetric and positive definite.

Property 2. From **Property 1** and (12), the inertia matrix $\mathbf{M_x(x_s)}$ is symmetric and positive definite, and it is known that

$$\lambda_{\min}\mathbf{I}\leq\mathbf{M}_\mathbf{x}\leq\lambda_{\max}\mathbf{I} \tag{17}$$

Property 3. The matrix $\dot{\mathbf{M}}_\mathbf{m}(\mathbf{x_m})-2\mathbf{C_m}(\mathbf{x_m},\dot{\mathbf{x}}_\mathbf{m})$ is skew-symmetric.

Property 4. There exists a $k_r>0$ such that $\mathbf{C_m}(\mathbf{x_m},\dot{\mathbf{x}}_\mathbf{m})\dot{\mathbf{x}}_\mathbf{m}\leq k_r|\dot{\mathbf{x}}_\mathbf{m}|^2$ for all time t.

Assumption 1. The time delays $h_1(t)$ and $h_2(t)$ are bounded. Therefore, there exist positive scalars $\overline{h}_1$ and $\overline{h}_2$ such that $0\leq h_1(t)\leq\overline{h}_1$ and $0\leq h_2(t)\leq\overline{h}_2$ for all t.

Assumption 2. The human operator and the environment behave in a non-passive way [25] and they are represented by the following model.

$$\mathbf{f_h}=-\alpha_h\dot{\mathbf{x}}_\mathbf{m}+\mathbf{f}_{\mathbf{a_h}} \tag{18}$$

$$\mathbf{f_e}=-\alpha_e\dot{\mathbf{x}}_\mathbf{s}+\mathbf{f}_{\mathbf{a_e}} \tag{19}$$

where α_h is the damping of the human operator model, and α_e is the environment's damping (passive components). On the other hand, $\mathbf{f}_{\mathbf{a_h}}, \mathbf{f}_{\mathbf{a_e}}\in L_\infty$ involve non-passive and additional passive components and their bounds are given by $|\mathbf{f}_{\mathbf{a_h}}|\leq\overline{\mathbf{f}}_{\mathbf{a_h}}$ and $|\mathbf{f}_{\mathbf{a_e}}|\leq\overline{\mathbf{f}}_{\mathbf{a_e}}$, with $\overline{\mathbf{f}}_{\mathbf{a_h}}$ and $\overline{\mathbf{f}}_{\mathbf{a_e}}$ positive constants.

Lemma 1. [2]: For real vector functions $\mathbf{a}(.)$ and $\mathbf{b}(.)$ and a time-varying scalar $h(t)$ with $0\leq h(t)\leq\overline{h}$, the following inequality holds,

$$\begin{aligned}&-2\mathbf{a}^T(t)\int_{t-h(t)}^{t}\mathbf{b}(\xi)d\xi-\int_{t-h(t)}^{t}\mathbf{b}^T(\xi)\mathbf{b}(\xi)d\xi\\&\leq h(t)\mathbf{a}^T(t)\mathbf{a}(t)\leq\overline{h}\,\mathbf{a}^T(t)\mathbf{a}(t)\end{aligned} \tag{20}$$

Lemma 2. Considering Property 1, equation (11), (12) and (16), if $\mathbf{J}$ from (17) has full rank, the following equality holds

$$\mathbf{J}\overline{\mathbf{M}}_\mathbf{s}^{\ -1}\mathbf{N}^\mathbf{T}=0 \tag{21}$$

Proof. Combining equations (11) and (16)

$$\mathbf{N^T}=\mathbf{I}-\mathbf{J^T}\mathbf{M_x}\mathbf{J}\overline{\mathbf{M}}_\mathbf{s}^{-1} \tag{22}$$

pre multiplying (22) by $\mathbf{J}\overline{\mathbf{M}}_\mathbf{s}^{-1}$

$$\mathbf{J}\overline{\mathbf{M}}_\mathbf{s}^{-1}\mathbf{N^T}=\mathbf{J}\overline{\mathbf{M}}_\mathbf{s}^{-1}-\mathbf{J}\overline{\mathbf{M}}_\mathbf{s}^{-1}\mathbf{J^T}\mathbf{M_x}\mathbf{J}\overline{\mathbf{M}}_\mathbf{s}^{-1} \tag{23}$$

From relation (12) $\mathbf{M_x}^{-1}= \mathbf{J}\overline{\mathbf{M}}_\mathbf{s}^{-1}\mathbf{J^T}$, substituting in equation (23) it is proved that $\mathbf{J}\overline{\mathbf{M}}_\mathbf{s}^{-1}\mathbf{N^T} = 0$.

In the next section, the control scheme will be introduced.

III. PD-LIKE CONTROLLER FOR TELEOPERATION

PD-like controllers are simple structures that have a good performance in practice for many applications and their parameters are calibrated quickly. Recently, the performance of these schemes has been evaluated for the position and velocity control of bilateral teleoperation systems of manipulator and mobile robots [10,11]. In these cases, if the damping of the master and slave are sufficiently big, then stability is assured.

Here, the teleoperation system is used to control the velocity of the end effector of a mobile manipulator, where the user permanently sends commands and perceives by means of force feedback the remote task. A force PD-like scheme is used in the task space in order to ensure teleoperation stability, but as the slave robot is redundant, the joint torque vector that produces a desired operational force is not unique (15). Then, a local loop is necessary to ensure reference tracking considering the high-coupled dynamics, as well as take advantage of the motion redundancy to reach secondary control objectives, such as posture control, obstacles avoidance or manipulability maximization among others, without affecting the end effector velocity.

The PD-like controller proposed establishes the control actions as follows,

$$\begin{cases} \mathbf{f_m} = -k_m\left(k_g\mathbf{x_m} - \dot{\mathbf{x}}_\mathbf{s}(t-h_2)\right) - \alpha_m\dot{\mathbf{x}}_\mathbf{m} - k_p\mathbf{x_m} + \mathbf{g_m} \\ \tau_\mathbf{c} = \mathbf{J^T}\left(\varsigma - \mathbf{M_x}\dot{\mathbf{J}}v\right) + \mathbf{N^T}\boldsymbol{\tau}_\mathbf{o} + \overline{\mathbf{C}}_\mathbf{s}(\mathbf{q},\dot{\mathbf{q}})\mathbf{v} + \overline{\mathbf{g}}_\mathbf{s}(\mathbf{q}) \\ \varsigma = k_s\left(k_g\mathbf{x_m}(t-h_1) - \dot{\mathbf{x}}_\mathbf{s}\right) - \sigma_s\mathbf{z} \end{cases} \tag{24}$$

Where the controller is formed by $\mathbf{f_m}$ and $\boldsymbol{\tau}_\mathbf{c}$. The parameters $\mathbf{k_s}$ and $\boldsymbol{\sigma}_\mathbf{s}$ are a positive constant that represents the proportional gain and acceleration dependent damping added by the velocity controller, $\alpha_\mathbf{m}$,$\mathbf{k_p}$ are the damping and spring injected in the master, and $\mathbf{k_m}$ represents a relative spring depending on the mismatch between the master reference and the robot velocity. Besides, the parameter $\mathbf{k_g}$ maps the master position to a velocity reference, and $\mathbf{z}$ is an auxiliary variable that represents measured mobile robot acceleration $\ddot{\mathbf{x}}_\mathbf{s}$

$$\ddot{\mathbf{x}}_\mathbf{s} = \mathbf{z} \tag{25}$$

Besides, $\boldsymbol{\tau}_\mathbf{o}$ is the null space control action, which will be taken into account to achieve any secondary tasks. Next, the stability of the delayed bilateral teleoperation system is modeled by (1),(10),(18),(19), the communication channel, featured by Assumption 1 and the PD-like controller (24) will be analyzed.

Remark 1. It is important to signal that the whole system is nonlinear and includes asymmetric time-varying delays.

Remark 2. The control scheme does not compensate the non-modeled external forces but they are felt by the human operator since such forces, represented by the term $\mathbf{f}_{\mathbf{e}^\mathbf{a}}$ in (19), change the end effector motion and therefore the force feedback received by the user.

IV. STABILITY OF THE DELAYED CLOSED-LOOP SYSTEM

The stability analysis of the control scheme is based on a Lyapunov-Krasovskii functional (LKF) [26] applied to bilateral teleoperation of a mobile manipulator . Now, we present the main result of this work as follows.

Theorem 1. Consider a delayed teleoperation system, where a human operator (18) using a master device (1) drives a remote non-holonomic mobile manipulator robot described by (10) interacting with an environment (19), and where the control law (24) is included. For positive constant parameters k_m, k_s, k_g, l, p considering Assumptions **1**, **2** and Properties **1**, **2, 3** and **4**; if the control parameters α_m and σ_s are such that the following inequalities hold:

$$\begin{aligned} \lambda_m &= k_g(\alpha_m + \alpha_h) - k_g l\overline{h}_1 - \overline{h}_2\frac{{k_g}^2{k_m}^2}{4p} > 0 \\ \lambda_s &= \frac{k_m\sigma_s}{k_s} - p\overline{h}_2 - \frac{\overline{h}_1 k_g {k_m}^2}{4l} > 0 \end{aligned} \tag{26}$$

Then the vector $\mathbf{x} = \left[\mathbf{x_m}\,\dot{\mathbf{x}}_\mathbf{m}\,k_g\mathbf{x_m} - \dot{\mathbf{x}}_\mathbf{s}\,\mathbf{z}\,\dot{\mathbf{x}}_\mathbf{s}\right]^\mathbf{T} \in L_\infty$. In addition, the variables $\dot{\mathrm{x}}_\mathrm{m}$ and $\mathbf{z}$ are ultimately bounded to a convergence zone established by $\frac{\rho_m}{\lambda_m}$ and $\frac{\rho_s}{\lambda_s}$ respectively, where $\rho_m = k_g\overline{\mathbf{f}}_{\mathbf{a_h}}$ and $\rho_s = k_m{k_s}^{-1}\overline{\mathbf{f}}_{\mathbf{a_e}}$.

Proof. First, a functional $V = V_1 + V_2 + V_3 + V_4 + V_5 + V_6 > 0$ is proposed in order to analyze its evolution along the system trajectories. It is formed by six parts: V_1 represents the kinetic energy of the master, V_2 considers the potential energy of the error between the master and the slave robot, V_3, V_4 taking into account the motion energy of the mobile manipulator, V_5 represents the potential energy of the master, and V_6 is included for mathematical reasons in order to transform the terms that include delayed variables to terms with non-delayed variables. The sub-functional are defined in the following manner:

$$V_1 = \frac{1}{2} k_g \dot{\mathbf{x}}_\mathbf{m}^{\mathbf{T}} \mathbf{M}_\mathbf{m}(\mathbf{q}_\mathbf{m}) \dot{\mathbf{x}}_\mathbf{m} \tag{27}$$

$$V_2 = \frac{1}{2} k_m \left(k_g \mathbf{x}_\mathbf{m} - \dot{\mathbf{x}}_\mathbf{s}\right)^{\mathbf{T}} \left(k_g \mathbf{x}_\mathbf{m} - \dot{\mathbf{x}}_\mathbf{s}\right) \tag{28}$$

$$V_3 = \frac{1}{2} \alpha_e k_m k_s^{-1} \dot{\mathbf{x}}_\mathbf{s}^{\mathbf{T}} \dot{\mathbf{x}}_\mathbf{s} \tag{29}$$

$$V_4 = k_m k_s^{-1} \int_0^t \mathbf{z}^{\mathbf{T}} \mathbf{M}_\mathbf{x} \mathbf{z}\, dt \tag{30}$$

$$V_5 = \frac{1}{2} k_p k_g \mathbf{x}_\mathbf{m}^{\mathbf{T}} \mathbf{x}_\mathbf{m} \tag{31}$$

$$\begin{aligned} V_6 = {} & p \int_{-\bar{h}_2}^{0} \int_{t+\theta}^{t} \mathbf{z}(\xi)^{\mathbf{T}} \mathbf{z}(\xi) d\,\xi d\theta \\ & + k_g l \int_{-\bar{h}_1}^{0} \int_{t+\theta}^{t} \dot{\mathbf{x}}_\mathbf{m}(\xi)^{\mathbf{T}} \dot{\mathbf{x}}_\mathbf{m}(\xi) d\,\xi d\,\theta \end{aligned} \tag{32}$$

The time derivative of (27) along the master dynamics (1) taking into account Properties **1** and **3**, is the following one,

$$\dot{V}_1 = k_g \frac{1}{2} \dot{\mathbf{x}}_\mathbf{m}^{\mathbf{T}} \dot{\mathbf{M}}_\mathbf{m} \dot{\mathbf{x}}_\mathbf{m} + k_g \dot{\mathbf{x}}_\mathbf{m}^{\mathbf{T}} \mathbf{M}_\mathbf{m} \ddot{\mathbf{x}}_\mathbf{m} \tag{33}$$

The local close loop dynamics of the master side is obtained replacing (24) and (18) in (1)

$$\begin{aligned} \mathbf{M}_\mathbf{m} \ddot{\mathbf{x}}_\mathbf{m} = {} & k_m \dot{\mathbf{x}}_\mathbf{s}(t - h_2) - k_m k_g \mathbf{x}_\mathbf{m} \\ & - (\alpha_m + \alpha_h) \dot{\mathbf{x}}_\mathbf{m} + \mathbf{f}_{\mathbf{a_h}} - \mathbf{C}_\mathbf{m} \dot{\mathbf{x}}_\mathbf{m} \end{aligned} \tag{34}$$

As $\dot{\mathbf{x}}_\mathbf{s}(t - h_2) = \dot{\mathbf{x}}_\mathbf{s}(t) - \int_{t-h_2}^{t} \ddot{\mathbf{x}}_\mathbf{s}(\xi) d\xi$, equation (34) can be written in the form (35)

$$\begin{aligned} \mathbf{M}_\mathbf{m} \ddot{\mathbf{x}}_\mathbf{m} = {} & - k_m \left(k_g \mathbf{x}_\mathbf{m} - \dot{\mathbf{x}}_\mathbf{s}\right) - k_m \int_{t-h_2}^{t} \ddot{\mathbf{x}}_\mathbf{s}(\xi) d\xi \\ & - (\alpha_m + \alpha_h) \dot{\mathbf{x}}_\mathbf{m} + \mathbf{f}_{\mathbf{a_h}} - \mathbf{C}_\mathbf{m} \dot{\mathbf{x}}_\mathbf{m} - k_p \mathbf{x}_\mathbf{m} \end{aligned} \tag{35}$$

Now, including (35) in (33) it yields,

$$\begin{aligned} \dot{V}_1 = {} & k_g \frac{1}{2} \dot{\mathbf{x}}_\mathbf{m}^{\mathbf{T}} \left(\dot{\mathbf{M}}_\mathbf{m} - 2\mathbf{C}_\mathbf{m}\right) \dot{\mathbf{x}}_\mathbf{m} - k_g k_m \dot{\mathbf{x}}_\mathbf{m}^{\mathbf{T}} \left(k_g \mathbf{x}_\mathbf{m} - \dot{\mathbf{x}}_\mathbf{s}\right) \\ & - k_g k_m \dot{\mathbf{x}}_\mathbf{m}^{\mathbf{T}} \int_{t-h_2}^{t} \ddot{\mathbf{x}}_\mathbf{s}(\xi) d\xi - (\alpha_m + \alpha_h) \dot{\mathbf{x}}_\mathbf{m} \\ & + k_g \dot{\mathbf{x}}_\mathbf{m}^{\mathbf{T}} \mathbf{f}_{\mathbf{a_h}} - k_g k_p \dot{\mathbf{x}}_\mathbf{m}^{\mathbf{T}} \mathbf{x}_\mathbf{m} \\ = {} & - k_g (\alpha_m + \alpha_h) \dot{\mathbf{x}}_\mathbf{m}^{\mathbf{T}} \dot{\mathbf{x}}_\mathbf{m} - k_g k_m \dot{\mathbf{x}}_\mathbf{m}^{\mathbf{T}} \left(k_g \mathbf{x}_\mathbf{m} - \dot{\mathbf{x}}_\mathbf{s}\right) \\ & - k_g k_m \dot{\mathbf{x}}_\mathbf{m}^{\mathbf{T}} \int_{t-h_2}^{t} \ddot{\mathbf{x}}_\mathbf{s}(\xi) d\xi + k_g \dot{\mathbf{x}}_\mathbf{m}^{\mathbf{T}} \mathbf{f}_{\mathbf{a_h}} - k_g k_p \dot{\mathbf{x}}_\mathbf{m}^{\mathbf{T}} \mathbf{x}_\mathbf{m} \end{aligned} \tag{36}$$

Then, $\dot{V}_2$ is obtained from (28) as follows,

$$\begin{aligned} \dot{V}_2 = {} & k_m \left(k_g \mathbf{x}_\mathbf{m} - \dot{\mathbf{x}}_\mathbf{s}\right)^{\mathbf{T}} \left(k_g \dot{\mathbf{x}}_\mathbf{m} - \ddot{\mathbf{x}}_\mathbf{s}\right) \\ = {} & k_g k_m \left(k_g \mathbf{x}_\mathbf{m} - \dot{\mathbf{x}}_\mathbf{s}\right)^{\mathbf{T}} \dot{\mathbf{x}}_\mathbf{m} - k_m \left(k_g \mathbf{x}_\mathbf{m} - \dot{\mathbf{x}}_\mathbf{s}\right)^{\mathbf{T}} \ddot{\mathbf{x}}_\mathbf{s} \end{aligned} \tag{37}$$

On the other hand, $\dot{V}_3$ is computed from (29),

$$\dot{V}_3 = \alpha_e k_m k_s^{-1} \dot{\mathbf{x}}_\mathbf{s}^{\mathbf{T}} \ddot{\mathbf{x}}_\mathbf{s} \tag{38}$$

Next, the slave robot close loop is needed to compute $\dot{V}_4$. Substituting τ_c of (24) in (10):

$$\begin{aligned} \dot{\mathbf{v}} = {} & \overline{\mathbf{M}}_\mathbf{s}^{-1} \mathbf{J}^{\mathbf{T}} \left(\varsigma - \mathbf{M}_\mathbf{x} \dot{\mathbf{J}} v\right) + \overline{\mathbf{M}}_\mathbf{s}^{-1} \mathbf{N}^{\mathbf{T}} \tau_\mathbf{o} \\ & + \overline{\mathbf{M}}_\mathbf{s}^{-1} \tau_{ve} \end{aligned} \tag{39}$$

Replacing (39) into (8) and then considering (12) in the resulting equation, the end effectors acceleration $\ddot{\mathbf{x}}_\mathbf{s}$ can be expressed as

$$\ddot{\mathbf{x}}_\mathbf{s} = \mathbf{M}_\mathbf{x}^{-1} \varsigma + \mathbf{J} \overline{\mathbf{M}}_\mathbf{s}^{-1} \mathbf{N}^{\mathbf{T}} \tau_\mathbf{o} + \mathbf{J} \overline{\mathbf{M}}_\mathbf{s}^{-1} \boldsymbol{\tau}_\mathbf{ve} \tag{40}$$

Besides, the operational space external force $\mathbf{f_e}$ in terms of joint space external torques $\boldsymbol{\tau}_\mathbf{ve}$ is

$$\mathbf{f_e} = \mathbf{J}^{+\mathbf{T}} \boldsymbol{\tau}_{ve} \tag{41}$$

Now, the acceleration produced by external torques in (40) can be expressed in terms of $\mathbf{f_e}$ pre multiplying (41) by $\mathbf{M}_\mathbf{x}^{-1}$ and taking into account (13)

$$\mathbf{M}_\mathbf{x}^{-1} \mathbf{f_e} = \mathbf{J} \overline{\mathbf{M}}_\mathbf{s}^{-1} \boldsymbol{\tau}_\mathbf{ve} \tag{42}$$

Inserting (42) and $\boldsymbol{\varsigma}$ from (24) into (40), and applying **Lemma 2** we get the slave robot closed loop dynamics in operation space.

$$\mathbf{M}_\mathbf{x} \ddot{\mathbf{x}}_\mathbf{s} = k_s k_g \mathbf{x}_\mathbf{m}(t - h_1) - k_s \dot{\mathbf{x}}_\mathbf{s} - \sigma_s \mathbf{z} + \mathbf{f_e} \tag{43}$$

Including $\mathbf{f_e}$ from (19) in (43) and considering that $\mathbf{x}_\mathbf{m}(t - h_1) = \mathbf{x}_\mathbf{m}(t) - \int_{t-h_1}^{t} \dot{\mathbf{x}}_\mathbf{m}(\xi) d\xi$, the slave device closed loop equation (44) is obtained.

$$\begin{aligned} \mathbf{M}_\mathbf{x} \ddot{\mathbf{x}}_\mathbf{s} = {} & - k_s k_g \int_{t-h_1}^{t} \dot{\mathbf{x}}_\mathbf{m}(\xi) d\xi - \alpha_e \dot{\mathbf{x}}_\mathbf{s} \\ & + k_s \left(k_g \mathbf{x}_\mathbf{m} - \dot{\mathbf{x}}_\mathbf{s}\right) - \sigma_s \mathbf{z} + \mathbf{f}_{\mathbf{a_e}} \end{aligned} \tag{44}$$

Now, $\dot{V}_4$ can be obtained inserting (44) into the derivative of (30), considering **Properties 1** and also the relation (25),

$$\begin{aligned}\dot{V}_4 &= k_m k_s{}^{-1}\mathbf{z}^{\mathbf{T}}\mathbf{M}_{\mathbf{x}}\mathbf{z}\\ &= k_m k_s{}^{-1}\mathbf{z}^{\mathbf{T}}\mathbf{M}_{\mathbf{x}}\ddot{\mathbf{x}}_{\mathbf{s}}\\ &= -k_m k_g\mathbf{z}^{\mathbf{T}}\int_{t-h_1}^{t}\dot{\mathbf{x}}_{\mathbf{m}}(\xi)d\xi - k_m k_s{}^{-1}\alpha_e\mathbf{z}^{\mathbf{T}}\dot{\mathbf{x}}_{\mathbf{s}}\\ &\quad + k_m\mathbf{z}^{\mathbf{T}}\left(k_g\mathbf{x}_{\mathbf{m}} - \dot{\mathbf{x}}_{\mathbf{s}}\right) - k_m k_s{}^{-1}\sigma_s\mathbf{z}^{\mathbf{T}}\mathbf{z}\\ &\quad + k_m k_s{}^{-1}\mathbf{z}^{\mathbf{T}}\mathbf{f}_{\mathbf{a_e}}\end{aligned} \tag{45}$$

Furthermore, $\dot{V}_5$ is obtained from (31) as follows,

$$\dot{V}_5 = k_p k_g\mathbf{x}_{\mathbf{m}}{}^{\mathbf{T}}\dot{\mathbf{x}}_{\mathbf{m}} \tag{46}$$

It is possible to appreciate in (36) and (45) that there are terms with delayed variables that make the stability analysis difficult. For solving this, V_6 is introduced. $\dot{V}_6$ is computed from (32), **Assumption 1** and Leibniz rule:

$$\begin{aligned}\dot{V}_6 \le & p\bar{h}_2\mathbf{z}^{\mathbf{T}}\mathbf{z} - p\int_{t-h_2}^{t}\mathbf{z}^{\mathbf{T}}(\xi)\mathbf{z}(\xi)d\xi\\ &+ k_g l\bar{h}_1\dot{\mathbf{x}}_{\mathbf{m}}{}^{\mathbf{T}}\dot{\mathbf{x}}_{\mathbf{m}} - k_g l\int_{t-h_1}^{t}\dot{\mathbf{x}}_{\mathbf{m}}{}^{\mathbf{T}}(\xi)\dot{\mathbf{x}}_{\mathbf{m}}(\xi)d\xi\end{aligned} \tag{47}$$

Next, $\dot{V} = \dot{V}_1 + \dot{V}_2 + \dot{V}_3 + \dot{V}_4 + \dot{V}_5 + \dot{V}_6$ is built joining (36), (37), (38), (45) and (47), and also considering the relation (25),

$$\begin{aligned}\dot{V} \le & -k_g(\alpha_m + \alpha_h)\dot{\mathbf{x}}_{\mathbf{m}}{}^{\mathbf{T}}\dot{\mathbf{x}}_{\mathbf{m}} + k_g l\bar{h}_1\dot{\mathbf{x}}_{\mathbf{m}}{}^{\mathbf{T}}\dot{\mathbf{x}}_{\mathbf{m}}\\ &- k_m k_s{}^{-1}\sigma_s\mathbf{z}^{\mathbf{T}}\mathbf{z} + p\bar{h}_2\mathbf{z}^{\mathbf{T}}\mathbf{z} + k_g\dot{\mathbf{x}}_{\mathbf{m}}{}^{\mathbf{T}}\mathbf{f}_{\mathbf{a_h}} + k_m k_s{}^{-1}\mathbf{z}^{\mathbf{T}}\mathbf{f}_{\mathbf{a_e}}\\ &- k_g k_m\mathbf{z}^{\mathbf{T}}\int_{t-h_1}^{t}\dot{\mathbf{x}}_{\mathbf{m}}(\xi)d\xi - k_g l\int_{t-h_1}^{t}\dot{\mathbf{x}}_{\mathbf{m}}{}^{\mathbf{T}}(\xi)\dot{\mathbf{x}}_{\mathbf{m}}(\xi)d\xi\\ &- k_m k_g\dot{\mathbf{x}}_{\mathbf{m}}{}^{\mathbf{T}}\int_{t-h_2}^{t}\mathbf{z}(\xi)d\xi - p\int_{t-h_2}^{t}\mathbf{z}^{\mathbf{T}}(\xi)\mathbf{z}(\xi)d\xi\end{aligned} \tag{48}$$

Using Lemma 1 (20) into the last terms of equation (48), relations (49) and (50) are established

$$\begin{aligned}&-k_g k_m\mathbf{z}^{\mathbf{T}}\int_{t-h_1}^{t}\dot{\mathbf{x}}_{\mathbf{m}}(\xi)d\xi - k_g l\int_{t-h_1}^{t}\dot{\mathbf{x}}_{\mathbf{m}}{}^{\mathbf{T}}(\xi)\dot{\mathbf{x}}_{\mathbf{m}}(\xi)d\xi\\ &= k_g l\left(-k_m l^{-1}\mathbf{z}^{\mathbf{T}}\int_{t-h_1}^{t}\dot{\mathbf{x}}_{\mathbf{m}}(\xi)d\xi - \int_{t-h_1}^{t}\dot{\mathbf{x}}_{\mathbf{m}}{}^{\mathbf{T}}(\xi)\dot{\mathbf{x}}_{\mathbf{m}}(\xi)d\xi\right)\\ &\le \frac{1}{4}\bar{h}_1 k_g k_m{}^2 l^{-1}\mathbf{z}^{\mathbf{T}}\mathbf{z}\end{aligned} \tag{49}$$

$$\begin{aligned}&-k_m k_g\dot{\mathbf{x}}_{\mathbf{m}}{}^{\mathbf{T}}\int_{t-h_2}^{t}\mathbf{z}(\xi)d\xi - p\int_{t-h_2}^{t}\mathbf{z}^{\mathbf{T}}(\xi)\mathbf{z}(\xi)d\xi\\ &= p\left(-k_g k_m p^{-1}\dot{\mathbf{x}}_{\mathbf{m}}{}^{\mathbf{T}}\int_{t-h_2}^{t}\mathbf{z}(\xi)d\xi - \int_{t-h_2}^{t}\mathbf{z}^{\mathbf{T}}(\xi)\mathbf{z}(\xi)d\xi\right)\\ &\le \frac{1}{4}\bar{h}_2 k_g{}^2 k_m{}^2 p^{-1}\dot{\mathbf{x}}_{\mathbf{m}}{}^{\mathbf{T}}\dot{\mathbf{x}}_{\mathbf{m}}\end{aligned} \tag{50}$$

Next (51) is derived applying relations (49) and (50) to (48) and regrouping terms.

$$\begin{aligned}\dot{V} &= \dot{V}_1 + \dot{V}_2 + \dot{V}_3 + \dot{V}_4 + \dot{V}_5 + \dot{V}_6\\ \dot{V} &\le -\dot{\mathbf{x}}_{\mathbf{m}}{}^{\mathbf{T}}\left(k_g(\alpha_m + \alpha_h)\mathbf{I} - k_g l\bar{h}_1\mathbf{I} - \bar{h}_2\frac{k_g{}^2 k_m{}^2}{4p}\mathbf{I}\right)\dot{\mathbf{x}}_{\mathbf{m}}\\ &\quad -\mathbf{z}^{\mathbf{T}}\left(\frac{k_m\sigma_s}{k_s}\mathbf{I} - p\bar{h}_2\mathbf{I} - \frac{\bar{h}_1 k_g k_m{}^2}{4l}\mathbf{I}\right)\mathbf{z}\\ &\quad + k_g\mathbf{f}_{\mathbf{a_h}}|\dot{\mathbf{x}}_{\mathbf{m}}| + \frac{k_m}{k_s}\mathbf{f}_{\mathbf{a_e}}|\mathbf{z}|\\ &= -\lambda_m\dot{\mathbf{x}}_{\mathbf{m}}{}^{\mathbf{T}}\dot{\mathbf{x}}_{\mathbf{m}} - \lambda_s\mathbf{z}^{\mathbf{T}}\mathbf{z} + \rho_s|\mathbf{z}| + \rho_m|\dot{\mathbf{x}}_{\mathbf{m}}|\end{aligned} \tag{51}$$

Given positive constant parameters for, k_m, k_s, k_g, l, and p as well as bounded values for $\bar{h}_1$, $\bar{h}_2$, $\bar{\mathbf{f}}_{\mathbf{a_e}}$ and $\bar{\mathbf{f}}_{\mathbf{a_h}}$, the control parameters α_m and σ_s can be set to guarantee that the first two terms of (51) are negative definite and therefore the variables $\dot{\mathbf{x}}_{\mathbf{m}}, \mathbf{z} \in L_\infty$. From this, it can be proved that $\left(k_g\mathbf{x}_{\mathbf{m}} - \dot{\mathbf{x}}_{\mathbf{s}}\right), \mathbf{x}_{\mathbf{m}}, \dot{\mathbf{x}}_{\mathbf{s}} \in L_\infty$ (see Appendix1) and therefore $\mathbf{x} = \left[\mathbf{x}_{\mathbf{m}} \quad \dot{\mathbf{x}}_{\mathbf{m}} \quad k_g\mathbf{x}_{\mathbf{m}} - \dot{\mathbf{x}}_{\mathbf{s}} \quad \mathbf{z} \quad \dot{\mathbf{x}}_{\mathbf{s}}\right]^{\mathbf{T}} \in L_\infty$. For this condition, it is possible to appreciate from (51) that the state variables

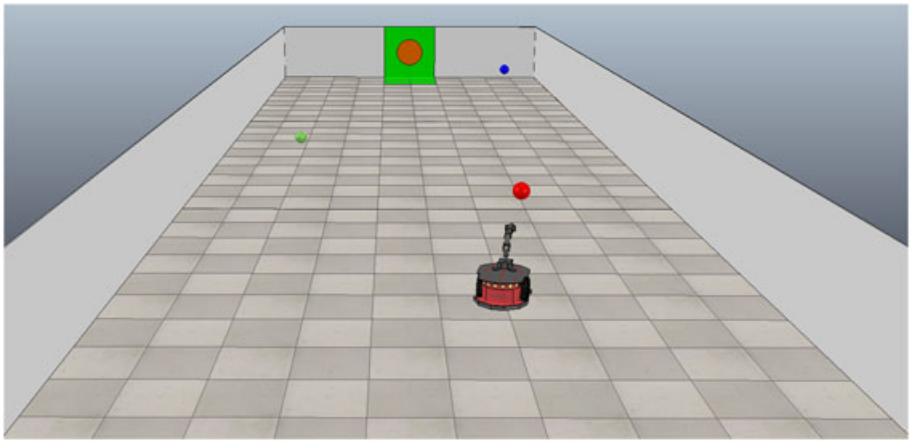

Fig. 1. 3D Inspection Task.

$\dot{\mathbf{x}}_\mathbf{m}$ and $\mathbf{z}$ are ultimately bounded to a convergence zone established by $\frac{\rho_m}{\lambda_m}$ and $\frac{\rho_s}{\lambda_s}$ respectively.

Remark 3. Positive constants l and p are design parameters that can be used to distribute damping between master device and slave robot in order to meet the technological limitations of them.

Remark 4. If the components of the human operator $\mathbf{f}_{\mathbf{a_h}}$ and environment $\mathbf{f}_{\mathbf{a_e}}$ are null $\left(\overline{\mathbf{f}}_{\mathbf{a_h}} = \overline{\mathbf{f}}_{\mathbf{a_e}}, = 0\right)$, then $\rho_m = \rho_s = 0$ and therefore the system is stable. For this particular case, the Barbalat's lemma can be used in (51) where taking into account Assumptions **1** to **2**, Property **1** to **4** and that $\mathbf{x_m}, \dot{\mathbf{x}}_\mathbf{m}, \left(k_g\mathbf{x_m} - \dot{\mathbf{x}}_\mathbf{s}\right), \mathbf{z}, \dot{\mathbf{x}}_\mathbf{s} \in L_\infty$, it is possible to deduce that $\ddot{\mathbf{x}}_\mathbf{m}$ and $\dot{\mathbf{z}}$ are bounded and therefore $\ddot{\mathbf{V}}$ is bounded too. Then $\ddot{\mathbf{x}}_\mathbf{m}$ and $\mathbf{z}$ will tend to zero as $t \to \infty$.

V. PARAMETERS ADJUSTMENT PROCEDURE

In this section a procedure for setting parameters is proposed to simplify the practical implementation of the system.

The parameters k_g, k_p, k_m, k_s, k_h, α_m, σ_s, δ, l, p in previous sections were taken as scalar, but in general they can be diagonal matrices called $\mathbf{K_g}, \mathbf{K_p}, \mathbf{K_m}, \mathbf{K_s}, \mathbf{K_h}, \boldsymbol{\alpha}_\mathbf{m}, \boldsymbol{\sigma}_\mathbf{s}, \mathbf{L}, \mathbf{P}$ respectively.

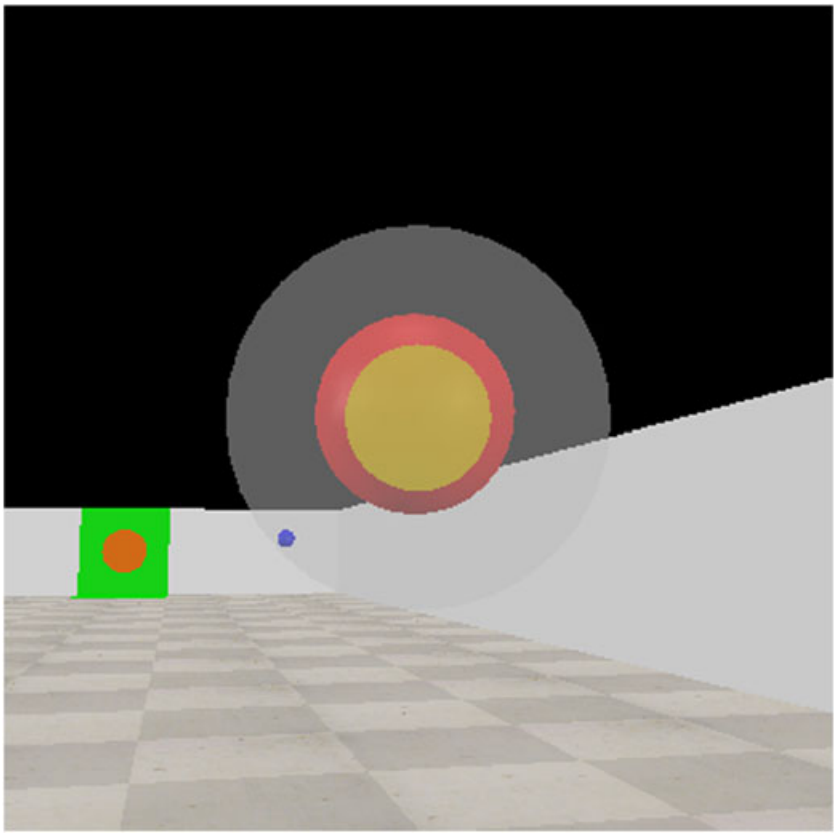

Fig. 2. Third task objective.

Table I. Experimental results in % of (59).

	Delay 1			Delay 2			Delay 3		
% of (53)	10%	100%	180%	10%	100%	180%	10%	100%	180%
$\%T_{task}$	144%	122%	151%	200%	146%	198%	267%	220%	259%
$\%\|\|I_e\|\|$	512%	354%	389%	764%	593%	673%	819%	707%	613%
$\%T_{task}\|\|I_e\|\|$	749%	434%	591%	1524%	872%	1330%	2187%	1566%	1590%

As stated in section III the variable $\mathbf{z}$ is a measurement of mobile robot acceleration $\ddot{\mathbf{x}}_\mathbf{s}$. On real systems the acceleration measurement is noisy then low pass filters are usually employed, such as

$$\ddot{\mathbf{x}}_\mathbf{s} = \mathbf{z} + \gamma\dot{\mathbf{z}} \tag{52}$$

with $\gamma \to 0^+$. For discrete time implementation $\mathbf{z}$ represents the mobile robot acceleration $\ddot{\mathbf{x}}_\mathbf{s}$ obtained in last sampling time k-1 previous to the current sample k.

Through the matrices $\mathbf{L}$ and $\mathbf{P}$ proposed in the theoretical analysis, different criteria can be used to establish a practical condition over system damping, that is, $\mathbf{L}$ and $\mathbf{P}$could be set to minimize damping injected to the system. We propose a conservative condition that is aimed to simplify equation (26) to a representative expression of the variables that influence the damping injection. Selecting $\mathbf{L} = \boldsymbol{\alpha}_\mathbf{m}\left(\overline{h}_1 + \overline{h}_2\right)^{-1} > 0$ and $\mathbf{P} = 1/4\boldsymbol{\alpha}_\mathbf{m}{}^{-1}\mathbf{K}_\mathbf{g}\mathbf{K}_\mathbf{m}{}^2\left(\overline{h}_1 + \overline{h}_2\right) > 0$, condition (26) is simplified to (53).

$$\begin{aligned} &\boldsymbol{\alpha}_\mathbf{h} \geq 0 \\ &\boldsymbol{\sigma}_\mathbf{s} \geq \frac{1}{4}\boldsymbol{\alpha}_\mathbf{m}{}^{-1}\mathbf{K}_\mathbf{s}\mathbf{K}_\mathbf{g}\mathbf{K}_\mathbf{m}\left(\overline{h}_1 + \overline{h}_2\right)^2 \end{aligned} \tag{53}$$

In this expression, the effect of parameters $\mathbf{K}_\mathbf{s}, \mathbf{K}_\mathbf{g}, \mathbf{K}_\mathbf{m}, \overline{h}_1, \overline{h}_2$ over system damping is clearer. Usually the master controller damping $\boldsymbol{\alpha}_\mathbf{m}$ is limited by the force capabilities of the master robot employed, while the slave damping $\boldsymbol{\sigma}_\mathbf{s}$ can be freely configured by the designer.

The following adjustment procedure and selection of parameters for the presented system is proposed.

a Taking $\mathbf{K}_\mathbf{m} = 0$(unilateral case), and $h_1 = h_2 = 0$, set $\mathbf{K}_\mathbf{g}$ to establish the maximum velocity command and $\mathbf{K}_\mathbf{s}$ considering the dynamics of the mobile robot so that a good performance of the velocity controller in the remote side is achieved. Choose γ value in (52) to remove noise from the measured acceleration signal $\ddot{\mathbf{x}}_\mathbf{s}$.
b Set $\mathbf{K}_\mathbf{m}$ to match the desired level of force feedback cue considering the different gains between the

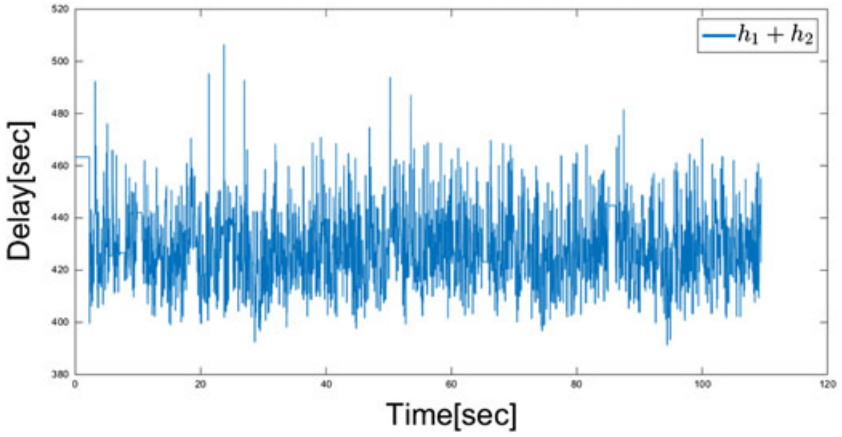

Fig. 3. Experiment total time delay.

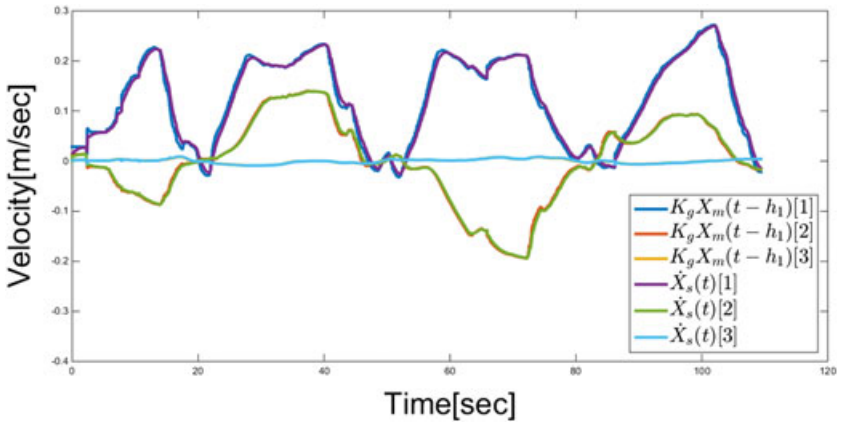

Fig. 4. Slave reference and end effector velocity.

master and mobile robot. $\mathbf{K_p}$ is chosen near zero to avoid interfering with the force feedback.

c Select $\boldsymbol{\alpha_m}$to meet the maximum force capabilities of the master device.

d From the values of $\mathbf{K_s}, \mathbf{K_g}, \mathbf{K_m}, \boldsymbol{\alpha_m}$, and taking into account the maximum communication channel delays $\overline{h}_1, \overline{h}_2$ determine the value of the slave robot damping by equation (53).

VI. HUMAN-IN-THE-LOOP SIMULATIONS

In this section experimental results are obtained. A human operator drives a simulator of a mobile Robot employing a Novint Falcon hand-controller with force feedback. The robots dynamics are simulated using Simulink, and visualization is done by V-REP. The aim of the experiment is to photograph spheres distributed in 3D space (Fig. 1), and the operator must fit each sphere within a predefined limit in the image plane (Fig. 2). This task cannot be accomplished with a traditional manipulator limited to its work area, nor can it be accomplished by a mobile robot limited by the plane of movement.

A posture control is applied to the null space control actions τ_o:

$$\tau_o = \mathbf{K_\rho}\left(\mathbf{p_{ref}} - \int_0^t \mathbf{v}(\xi)d\xi\right) - \mathbf{K_v}v - \mathbf{K_a}\dot{v} \tag{54}$$

Where $\mathbf{p_{ref}}$ is the desired posture of the mobile manipulator, $\mathbf{K}_\rho, \mathbf{K_v}$ and $\mathbf{K_a}$ are diagonal, positive defined matrices.

For the inspection task, it is desirable that the mobile manipulator keeps a posture with the elbows up, facilitating navigation. This can be achieved by setting the null space parameters high. Since the mass of the base is much higher than that of the manipulator, the latter robot is able to respond faster to sudden changes of the reference rate. If the parameters of the secondary posture controller are set very high, the arm will remain stiff and speed reference will be executed by the base, the responsiveness of which is lower. Then, the null space controller parameters (54) are adjusted empirically as a trade-off between speed of response and navigation posture (55).

$$\begin{aligned}
&\mathbf{K_\rho} = diag([0 \quad 0 \quad 5 \quad 5 \quad 5 \quad 5])\\
&\mathbf{K_v} = diag([5 \quad 5 \quad 5 \quad 5 \quad 5 \quad 5])\\
&\mathbf{K_a} = diag([0.1 \quad 0.1 \quad 0.1 \quad 0.1 \quad 0.1 \quad 0.1])\\
&\mathbf{K_g} = diag([7 \quad 1.2 \quad 0.2])\\
&\mathbf{K_m} = diag([20 \quad 50 \quad 200])\\
&\mathbf{p_{ref}} = [0 \quad 0 \quad 0 \quad \pi/4 \quad \pi/4 \quad 0]^T\\
&\gamma = 0.01, k_s = 70, \; k_p = 0.001
\end{aligned} \tag{55}$$

In this work, the time delays are taken in a general way as variables, asymmetric and with bounded magnitude. The system performance is tested locally for three different simulated time delays (56).

For these experiments $\boldsymbol{\alpha_m}$ was set to 110 [Kg/s] through all time delays tested and $\boldsymbol{\sigma_s}$ was calculated using (53) for a particular set of $\overline{h}_1$, $\overline{h}_2$, called Delay 1, Delay 2 and Delay 3, which are established explicitly in (51).

$$\begin{aligned}
&\text{Delay 1}: \begin{cases} h_1 = 0.25 + 0.05\sin(4t + 0.1) \\ h_2 = 0.29 + 0.01\sin(t + 0.5) \end{cases}\\
&\text{Delay 2}: \begin{cases} h_1 = 0.4 + 0.1\sin(4t + 0.1) \\ h_2 = 0.35 + 0.15\sin(t + 0.5) \end{cases}\\
&\text{Delay 3}: \begin{cases} h_1 = 0.6 + 0.15\sin(4t + 0.1) \\ h_2 = 0.65 + 0.1\sin(t + 0.5) \end{cases}
\end{aligned} \tag{56}$$

Three different indexes are used to measure system performance. The first metrics is called T_{task}, defined as the

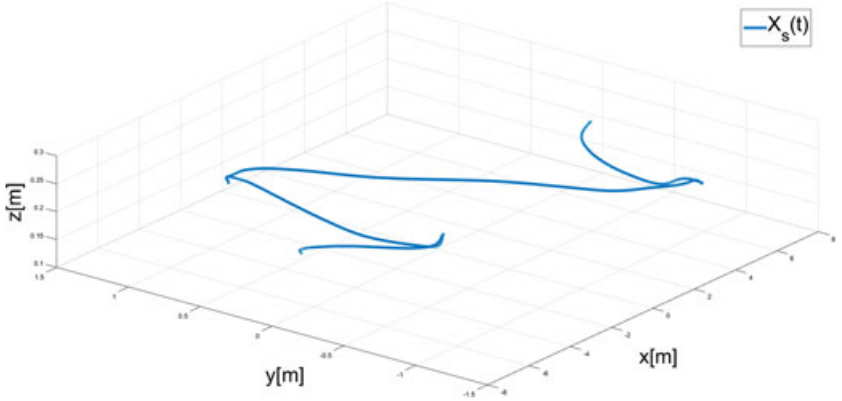

Fig. 5. End effector trajectory.

average time to complete each task, for a certain time delay and damping setting. This index is computed as follows:

$$T_{task} = \frac{1}{n}\sum_{i=1}^{n} t_{f_i} \tag{57}$$

where $n = 10$ is the test's quantity and t_{fi} is the time taken by the operator to complete the task in each test. The second index is synchronization error I_e which measures the average coupling between master and slave device. This metric is taken as stability index.

$$I_e = \frac{1000}{n}\sum_{i=1}^{n}\frac{1}{t_{f_i}}\int_0^{t_{f_i}} \left|k_g \mathbf{x}_{\mathbf{m}_i}(t) - \dot{\mathbf{x}}_{\mathbf{s}_i}(t)\right| dt \tag{58}$$

The third index is the product of indexes 1 and 2, and denotes a general criterion for assessing the performance of each setting.

Indexes are obtained for each time delay employing three damping settings for master and slave device, in % of the $\boldsymbol{\alpha}_{\mathbf{m}}$ chosen and $\boldsymbol{\sigma}_{\mathbf{s}}$ calculated.

Reference values are obtained considering $\overline{h}_1 = \overline{h}_2 = 0$ and $\boldsymbol{\alpha}_{\mathbf{m}} = \sigma_{\mathbf{s}} = 0$, for these settings the average performance index are:

$$\begin{cases} T_{task} = 65.49 \\ \|I_e\| = 4.37 \\ T_{task}\|I_e\| = 286.4 \end{cases} \tag{59}$$

Average results are presented in Table I as percentage of reference values given in (59).

It is important to note that the stability condition obtained in (26) is sufficient but not necessary. However, the experimental results exposed in Table I shows that when the damping is set weakly (10% of (59)), the indexes obtained are poor. On the other hand, an oversetting of damping does not improve all indexes. Even more, the calibration 100% of (59) produces the better index $\%T_{task}\|I_e\|$ for the time delays evaluated. Although a generalization of these results should include major quantity of experiments (different tasks, more types of time delay, more users, etc.), the parameters based on the theoretical analysis provide a good estimate of the adequate controller setting.

Next, the results of a teleoperation experiment via internet between Universidade Federal do Espírito Santo (UFES) of Vitoria ES, Brazil and Universidad Nacional de San Juan (UNSJ) of San Juan, Argentina, are presented.

The master device (Novint Falcon) is placed in UFES while the slave device (simulated mobile manipulator) is placed in UNSJ. The measured time delay of the experiment is shown in Fig. 3. The reference tracking of the slave control loop and the trajectory followed by the end effector of the mobile manipulator on the remote site are shown in Fig. 4. The mapped position of the slave device and the force feedback felt by the operator on the local site are included in Fig. 6. The Slave robot end effector velocity and torque applied to the mobile manipulator are shown in Fig. 7. Finally the synchronization error between master and slave robot is shown in Fig. 8.

In Fig. 5, the trajectory of the mobile manipulator end effector on the remote site, is shown. The robot inspects three objectives distributed in 3D space and then it goes to final zone marked in green (see Figure 1). From Figs 4–8 to 8 it is possible to appreciate that the main system variables remain bounded. Also in Fig. 4, the performance of the local slave controller can be seen, in which the slave robot is capable of accurately following the delayed reference of the remote control loop. Finally, the torques shown in Figs 6 and 7 are compatible with the capabilities of the master and slave robots, which for the Novint Falcon device is around 8.9 Newtons and for the mobile manipulator base is around 40 Newtons in its linear component.

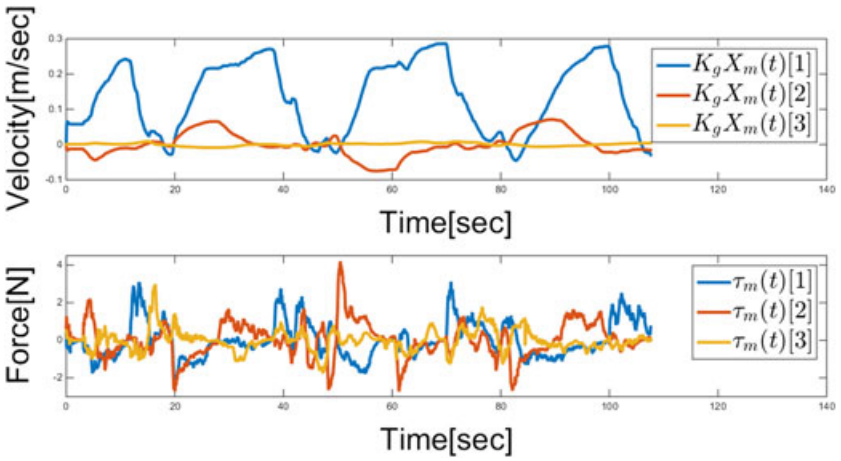

Fig. 6. Master reference and force feedback measured on local site.

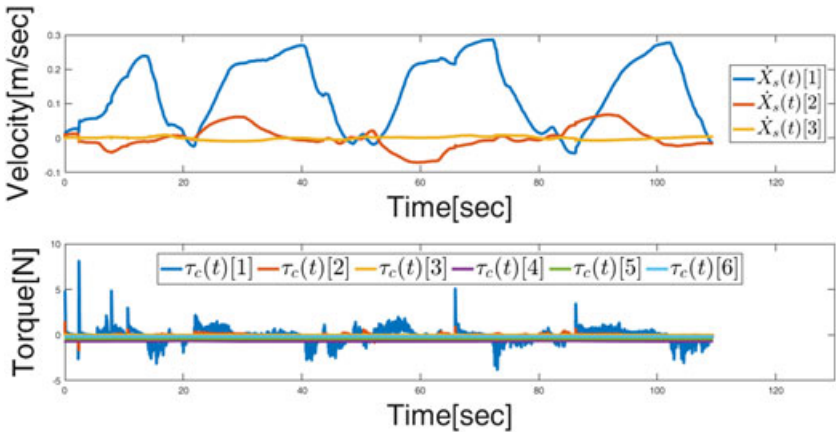

Fig. 7. Slave end effector velocity and applied torque measured on remote side.

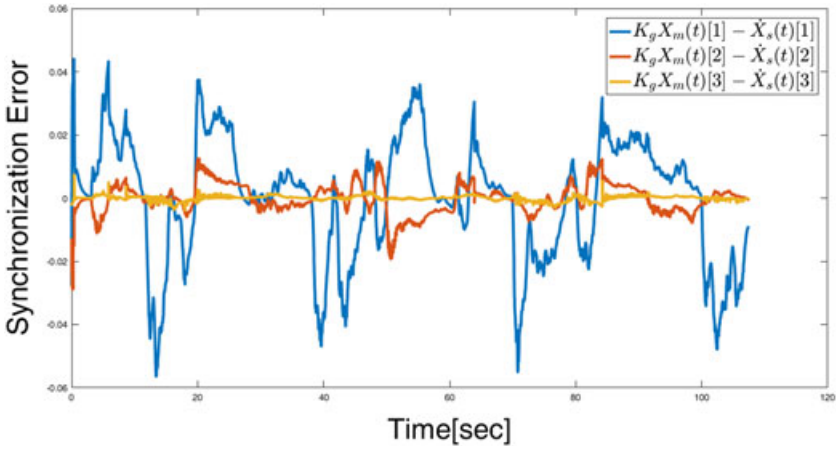

Fig. 8. Synchronization error between master and slave robot.

VII. CONCLUSIONS

In this paper, a stable scheme for bilateral teleoperation of a mobile manipulator has been proposed. The strategy includes a task space PD-like controller with damping injection and dynamic compensation on both master and slave robot. In addition, a redundancy resolution strategy based on operational space formulation was added. The stability analysis gives as its result a procedure for calibrating system parameters in compliance with the technological limitations of the devices. In addition, human-in-the-loop simulations were made. The task performance for different time delays and calibration of parameters was analyzed, concluding that the obtained results are in agreement with theoretical results achieved. Finally, a teleoperation experiment between Brazil and Argentina is presented to motivate the application potential of this type of system via the Internet to several areas.

REFERENCES

1. Sheridan, T., *Telerobotics, Automation, and Human Supervisory Control*, MIT Press, Cambridge, MA (1992).
2. Ferre, M., M. Buss, R. Aracil, C. Melchiorri, and C. Balaguer, *Advances in Telerobotics*, Springer, Heidelberg, Berlin (2007).
3. Hokayem, P. F., and M. W. Spong, "Bilateral teleoperation: An historical survey," *Automatica*, Vol. 42, No. 12, pp. 2035–2057 (2006).
4. Richard J.-P., "Time-delay systems: An overview of some recent advances and open problems," *Automatica,* Vol. 39, No. 10, pp.1667–1694 (2003).
5. Lawrence, D. A., "Stability and transparency in bilateral teleoperation," *IEEE Trans. Robot. Autom.*, Vol. 9, No. 5, pp. 624–637 (1993).
6. Varkonyi, T. A., I. J. Rudas, P. Pausits, and T. Haidegger, "Survey on the control of time delay

teleoperation systems," *Proc. 18th IEEE Int. Conf. Intell. Eng. Syst.,* Tihany, Hungary, pp. 89–94 (2014).
7. Niemeyer, G., and J.-J. Slotine, "Stable adaptive teleoperation," *IEEE J. Ocean. Eng.*, Vol. 16, No. 1, pp. 152–162 (1991).
8. Niemeyer, G., and J.-J. E. Slotine, "Telemanipulation with time delays," *Int. J. Robot. Res.*, Vol. 23, No. 9, pp. 873–890 (2004).
9. Anderson, R. J., and M. W. Spong, "Bilateral control of teleoperators with time delay," *IEEE Trans. Autom. Control*, Vol. 34, No. 5, pp. 494–501 (1989).
10. Nuno, E., R. Ortega, N. Barabanov, and L. Basanez, "A globally stable PD controller for bilateral teleoperators," *IEEE Trans. Robot.*, Vol. 24, No. 3, pp.753–758 (2008).
11. Hua, C.-C., and X. P. Liu, "Delay-dependent stability criteria of teleoperation systems with asymmetric time-varying delays," *IEEE Trans. Robot.*, Vol. 26, No. 5, pp. 925–932 (2010).
12. Slawiñski, E., and V. Mut, "PD-like controllers for delayed bilateral teleoperation of manipulators robots," *Int. J. Robust Nonlinear Control.*, Vol. 25, No. 12, pp. 1801–1815 (2015).
13. Hirche, S., and M. Buss, "Human-oriented control for haptic teleoperation," *Proc. IEEE*, Vol. 100, No. 3, pp. 623–647 (2012).
14. Farkhatdinov, I., J.-H. Ryu, and J. Poduraev, "A feasibility study of time-domain passivity approach for bilateral teleoperation of mobile manipulator," *Proc. Int. Conf. Control, Autom. Syst.*, Seoul, Korea, pp. 272–277 (2008).
15. Farkhatdinov, I. and J.-H. Ryu, "Switching of control signals in teleoperation systems: Formalization and application," *Proc. IEEE/ASME Int. Conf. Adv. Intell. Mechatronics.*, Xian, China, pp. 353–358 (2008).
16. Lasnier, A. and T. Murakami, "Hybrid sensorless bilateral teleoperation of two-wheel mobile manipulator with underactuated joint," *Proc. IEEE/ASME Int. Conf. Adv. Intell. Mechatronics.*, Montreal, Canada, pp. 347–352 (2010).
17. Andaluz, V. H., L. Salinas, F. Roberti, J. M. Toibero, and R. Carelli, "Switching control signal for bilateral tele-operation of a mobile manipulator," *Proc. 9th IEEE Int. Conf. Control Autom.*, Santiago, Chile, pp.778–783 (2011).
18. Park, J., and O. Khatib, "A haptic teleoperation approach based on contact force control," *Int. J. Robot. Res.*, Vol. 25, No. 5–6, pp. 575–591 (2006).
19. Park, J., and O. Khatib, "Robust haptic teleoperation of a mobile manipulation platform," In *Experimental Robotics IX*, Springer, Berlin, pp. 543–554 (2006).
20. Khatib, O., "A unified approach for motion and force control of robot manipulators: The operational space formulation," *IEEE J. Robot. Autom.*, Vol. 3, No. 1, pp. 43–53 (1987).
21. Sciavicco, L., and B. Siciliano, *Modelling and Control of Robot Manipulators*, Springer Science & Business Media, London, UK (2000).
22. Li, Z., and S. S. Ge, *Fundamentals in Modeling and Control of Mobile Manipulators*, CRC Press, FL, USA (2013).
23. Hu, M. and B. H. Guo, "Modeling and motion planning of a three-link wheeled mobile manipulator," *Proc. 8th Control Autom. Robot. Vision Conf.*, *2004.,* Kunming, China, Vol. 2, pp. 993–998 (2004).
24. Khatib, O., "Commande dynamique dans l'espace opérationnel des robots manipulateurs en présence d'obstacles," PhD thesis, École Nationale Supérieure de l'Aeronautique et de l'Espace (ENSAE), Toulouse, France (1980).
25. Islam, S., Liu, P. X., El Saddik, A., Dias, J., and L. Seneviratne, "Bilateral shared autonomous systems with passive and nonpassive input forces under time varying delay," *ISA Trans.*, Vol. 54, pp. 218–228 (2015).
26. Fridman, E., "Tutorial on Lyapunov-based methods for time-delay systems," *Eur. J. Control*, Vol. 20, No. 6, pp. 271–283 (2014).

APPENDIX 1

Next the boundedness of system states $(k_g\mathbf{x_m} - \dot{\mathbf{x}}_\mathbf{s}), \mathbf{x_m}, \dot{\mathbf{x}}_\mathbf{s}$will be analyzed.

From theorem 1 the variables $\dot{\mathbf{x}}_\mathbf{m}, \mathbf{z}$are bounded $\forall t$, that is

$$\begin{aligned} &|\dot{\mathbf{x}}_\mathbf{m}| \le \beta_{\dot{\mathbf{x}}_\mathbf{m}} \\ &|\mathbf{z}| \le \beta_\mathbf{z} \end{aligned} \tag{60}$$

From last relations, the following inequalities, which will be used below, can be written as

$$\begin{aligned} &\left|\int_{t-h_1}^{t} \dot{\mathbf{x}}_\mathbf{m}(\xi)d\xi\right| \le \sup_{\xi\in[t-h_1,t]} |\dot{\mathbf{x}}_\mathbf{m}(\xi)| \int_{t-h_1}^{t} d\xi \le \overline{h}_1 \beta_{\dot{\mathbf{x}}_\mathbf{m}} \\ &\left|\int_{t-h_2}^{t} \mathbf{z}(\xi)d\xi\right| \le \sup_{\xi\in[t-h_2,t]} |\mathbf{z}(\xi)| \int_{t-h_2}^{t} d\xi \le \overline{h}_2 \beta_\mathbf{z} \end{aligned} \tag{61}$$

By clearing $\dot{\mathbf{x}}_\mathbf{s}$ in equation (44) and replacing its expression in equation (35), the whole system closed loop equation is obtained, which can be written by convenience in the form (62).

$$\mathbf{M_m}\ddot{\mathbf{x}}_\mathbf{m} + \mathbf{C}_2\dot{\mathbf{x}}_\mathbf{m} + \mathbf{C}_1\mathbf{x_m} = f(\mathbf{x}) \tag{62}$$

where

$$\mathbf{C}_1 = \left(k_p + k_g k_m\left(1 - \frac{k_s}{\alpha_e + k_s}\right)\right)\mathbf{I} > 0$$
$$\mathbf{C}_2 = (\alpha_m + \alpha_h)\mathbf{I} > 0$$
$$f(\mathbf{x}) = -\frac{k_s k_g k_m}{\alpha_e + k_s}\int_{t-h_1}^{t} \dot{\mathbf{x}}_\mathbf{m}(\xi)d\xi - \frac{k_m}{\alpha_e + k_s}\mathbf{M}_\mathbf{x}\ddot{\mathbf{x}}_\mathbf{s} - \frac{k_m\sigma_s}{\alpha_e + k_s}\mathbf{z} + k_m(\alpha_e + k_s)^{-1}\mathbf{f}_{\mathbf{a_e}} + \mathbf{f}_{\mathbf{a_h}} - k_m\int_{t-h_2}^{t} \ddot{\mathbf{x}}_\mathbf{s}(\xi)d\xi - \mathbf{C}_\mathbf{m}\dot{\mathbf{x}}_\mathbf{m}$$

Applying Minkowski inequality to $|f(\mathbf{x})|$ considering bounded values (60),(61) and equation (25), the following relation is achieved:

$$f(\mathbf{x}) \le \frac{k_s k_g k_m}{\alpha_e + k_s}\bar{h}_1\beta_{\dot{\mathbf{x}}_\mathbf{m}} + \frac{k_m}{\alpha_e + k_s}|\mathbf{M}_\mathbf{x}|\beta_\mathbf{z} + \frac{k_m\sigma_s}{\alpha_e + k_s}\beta_\mathbf{z} + k_m(\alpha_e + k_s)^{-1}\bar{\mathbf{f}}_{\mathbf{a_e}} + \bar{\mathbf{f}}_{\mathbf{a_h}} + k_m\bar{h}_2\beta_\mathbf{z} + k_r{\beta_{\dot{\mathbf{x}}_\mathbf{m}}}^2 \tag{63}$$

Next, Property 2 is applied to (63). The following expression is reached,

$$f(\mathbf{x}) \le \beta_1\mathbf{I} \tag{64}$$

where $\beta_1 \in L_\infty$ is given by

$$\beta_1 = \frac{k_s k_g k_m\bar{h}_1\beta_{\dot{\mathbf{x}}_\mathbf{m}}}{\alpha_e + k_s} + k_r{\beta_{\dot{\mathbf{x}}_\mathbf{m}}}^2 + \frac{k_m}{\alpha_e + k_s}\bar{\mathbf{f}}_{\mathbf{a_e}} + \frac{k_m\sigma_s\beta_\mathbf{z}}{\alpha_e + k_s} + \frac{k_m\lambda_{\max}\beta_\mathbf{z}}{\alpha_e + k_s} + k_m\bar{h}_2\beta_\mathbf{z} + \bar{\mathbf{f}}_{\mathbf{a_h}}$$

From equation (62) and (64) we can express that $\mathbf{M}_\mathbf{m}\ddot{\mathbf{x}}_\mathbf{m} + \mathbf{C}_2\dot{\mathbf{x}}_\mathbf{m} + \mathbf{C}_1\mathbf{x}_\mathbf{m} \le \beta_1\mathbf{I}$ where $\mathbf{M}_\mathbf{m}, \mathbf{C}_2, \mathbf{C}_1\mathbf{x}_\mathbf{m}$, $\beta_1\mathbf{I} > 0$ therefore $\mathbf{x}_\mathbf{m} \in L_\infty$. That is there exists $\beta_{\mathrm{xm}} > 0$ such that

$$|\mathbf{x}_\mathbf{m}| \le \beta_{\mathbf{x}_\mathbf{m}} \tag{65}$$

Next, an expression for $|\dot{\mathbf{x}}_\mathbf{s}|$ is obtained from (44),

$$(\alpha_e + k_s)|\dot{\mathbf{x}}_\mathbf{s}| = \left|-k_s k_g\int_{t-h_1}^{t} \dot{\mathbf{x}}_\mathbf{m}(\xi)d\xi - \mathbf{M}_\mathbf{x}\ddot{\mathbf{x}}_\mathbf{s} + k_s k_g\mathbf{x}_\mathbf{m} - \sigma_s\mathbf{z} + \mathbf{f}_{\mathbf{a_e}}\right| \tag{66}$$

Applying Minkowski inequality to (64), we have

$$(\alpha_e + k_s)|\dot{\mathbf{x}}_\mathbf{s}| \le k_s k_g\left|\int_{t-h_1}^{t} \dot{\mathbf{x}}_\mathbf{m}(\xi)d\xi\right| + |\mathbf{M}_\mathbf{x}\ddot{\mathbf{x}}_\mathbf{s}| + k_g k_s|\mathbf{x}_\mathbf{m}| + \sigma_s|\mathbf{z}| + |\mathbf{f}_{\mathbf{a_e}}| \tag{67}$$

Substituting bound values (60),(61) and (65) in (67) and applying Property 2, we get:

$$(\alpha_e + k_s)|\dot{\mathbf{x}}_\mathbf{s}| \le k_s k_g\bar{h}_1\beta_{\dot{\mathbf{x}}_\mathbf{m}} + (\lambda_{\max} + \sigma_s)\beta_\mathbf{z} + k_g k_s\beta_{\mathbf{x}_\mathbf{m}} + \bar{\mathbf{f}}_{\mathbf{a_e}} \tag{68}$$

Then $\dot{\mathbf{x}}_\mathbf{s} \in L_\infty$ with upper bound given by $\beta_{\dot{\mathbf{x}}_\mathbf{s}} = \frac{k_s k_g\bar{h}_1\beta_{\dot{\mathbf{x}}_\mathbf{m}} + k_g k_s\beta_{\mathbf{x}_\mathbf{m}} + (\lambda_{\max} + \sigma_s)\beta_\mathbf{z} + \bar{\mathbf{f}}_{\mathbf{a_e}}}{\alpha_e + k_s}$.

Analogously the signal $e = k_g\mathbf{x}_\mathbf{m} - \dot{\mathbf{x}}_\mathbf{s} \in L_\infty$ too. This signal has an upper bound given by $\beta_e = k_g\beta_{\mathbf{x}_\mathbf{m}} + \beta_{\dot{\mathbf{x}}_\mathbf{s}}$.

Diego D. Santiago graduated in Electronic Engineering from the National University of San Juan (UNSJ), Argentina in 2012. He currently works in the PhD program at the Automatic Control Institute (INAUT), Argentina. He also teaches computer programming in the Electronic Engineering career at UNSJ. His research areas are robotics, computer vision, software development, and teleoperation systems.

Emanuel Slawiñski was born in Comodoro Rivadavia Chubut, Argentina in 1975. He completed his undergraduate and postgraduate studies at the National University of San Juan (UNSJ) in Argentina, in 2001 and 2006 respectively. He is currently an associate professor in Electronic Engineering career at UNSJ, teaching in the field of robotics and control systems. In addition, he teaches robot control in the postgraduate program of UNSJ. Since 2008, he has been a scientific researcher at the National Council of Science and Technology (CONICET) in Argentina. His areas of work include robotics, teleoperation of robots, human–robot interaction, software development, sensory systems and haptic devices.

Vicente A. Mut is a professor at the National University of San Juan and an Independent Researcher at the National Council of Scientific and Technical Investigations of Argentina (CONICET), developing research activities and teaching at the graduate and posgraduate programs. He received his doctorate in engineering of systems of control from the National University of San Juan, Argentina in 1995. He has been qualified as Researcher Class I in the categorization for incentives program for research-education by the Argentinean government. His research interests are robotics, manufacturing systems, adaptive control and artificial intelligence applied to automatic control.